



# Prediction of the self-discharge profile of an electrochemical capacitor electrode in the presence of both activation-controlled discharge and charge redistribution

Jennifer Black, Heather A. Andreas\*

Department of Chemistry, Dalhousie University, Halifax, NS, Canada, B3H 4J3

## ARTICLE INFO

### Article history:

Received 27 June 2009

Received in revised form 14 August 2009

Accepted 17 August 2009

Available online 22 August 2009

### Keywords:

Self-discharge

Activation-controlled

Charge redistribution

Porous electrode

Electrochemical capacitors

Model pore

## ABSTRACT

In the porous electrodes typically used for electrochemical capacitors, the self-discharge profile may be affected by charge redistribution in the pores of the electrode and the kinetics of the Faradaic self-discharge. In this paper, the activation-controlled self-discharge of a porous electrode is modelled using a de Levie transmission line hardware circuit to model a pore and an activation-controlled discharge is applied at the mouth of this “pore”. The self-discharge profile exhibits three main regions. The first region is governed purely by the activation-controlled discharge as the charge redistribution has not yet begun. The second region combines both charge redistribution and the activation-controlled discharge, resulting in a shallower slope than expected for a purely activation-controlled discharge. Finally, charge redistribution ends and the profile reverts to the activation-controlled profile. These three regions are mirrored in experimental self-discharge profiles and show that the duration charge redistribution can be determined from the shape of the self-discharge profile.

© 2009 Elsevier B.V. All rights reserved.

## 1. Introduction

Electrochemical capacitors (ECs) are charge storage devices which in their most basic form store charge in an electrochemical double-layer formed at the electrode/electrolyte interface. The storage of charge in the double-layer results in lower energy-densities for ECs vs. that of fuel cells or batteries. To counter this, ECs are often manufactured with high surface area carbon electrodes. These high surface area electrodes allow for greater charge storage and therefore higher energy-densities.

During charging or discharging of these highly porous electrodes the potential at the tip of the pores (closest to the counter electrode) will change more quickly than the potential at the base of the pore (furthest from the counter electrode) due to the added solution resistance down the pores [1]. As a result, after charging (discharging) of an EC electrode there will be a distribution of potentials down the pores in the electrode surface. Upon switching the system to open-circuit there will be a redistribution of charge down the pores until all parts of the electrode surface are at an equal potential. In other words, after charging of a porous electrode the potential at the pore tip will fall (since the potential here will be the highest) and the potential at the pore base will climb until the entire pore is at an equal potential [2,3].

A hardware circuit, based on the de Levie transmission line model of a pore can be used to examine the potential profile of a pore during charging/discharging [1]. It has been shown that the charge redistribution (CR) throughout the pore after charging results in a linear potential profile in  $\log t$  [3]. This is the same profile predicted for a planar electrode undergoing activation-controlled (AC) self-discharge mechanism (Eq. (1))

$$V = -\frac{RT}{\alpha F} \ln \frac{\alpha F i_0}{RT C} - \frac{RT}{\alpha F} \ln \left[ t + \frac{C\tau}{i_0} \right] \quad (1)$$

where  $R$  is the universal gas constant,  $T$  is the temperature,  $\alpha$  is the transfer coefficient,  $F$  is Faraday's constant,  $i_0$  is the exchange current density,  $C$  is the capacitance,  $t$  is time, and  $\tau$  is an integration constant [4]. This model predicts a potential,  $V$ , decline with  $\ln t$  (or  $\log t$ ) with a slope that is the negative of the Tafel slope,  $RT/\alpha F$ , and suggests that an examination of the slope of the self-discharge curve may help in determining the mechanism through which self-discharge takes place. However, it should be noted that this model and equation was developed for a planar, not porous electrode. And, as shown previously in porous electrodes, like those often used in ECs, a linear profile seen in  $\log t$  is not necessarily indicative of an AC discharge mechanism and may rather be due to CR down the pores of the electrode after charging, or to some combination of both [3].

This work predicts the potential profile of an EC electrode undergoing an AC discharge in the presence of CR within the pores in order to identify the important characteristics of the potential profile and examine the effect of higher resistance and longer pores so

\* Corresponding author. Tel.: +1 902 494 4505. fax: +1 902 494 1310.  
E-mail address: [heather.andreas@dal.ca](mailto:heather.andreas@dal.ca) (H.A. Andreas).

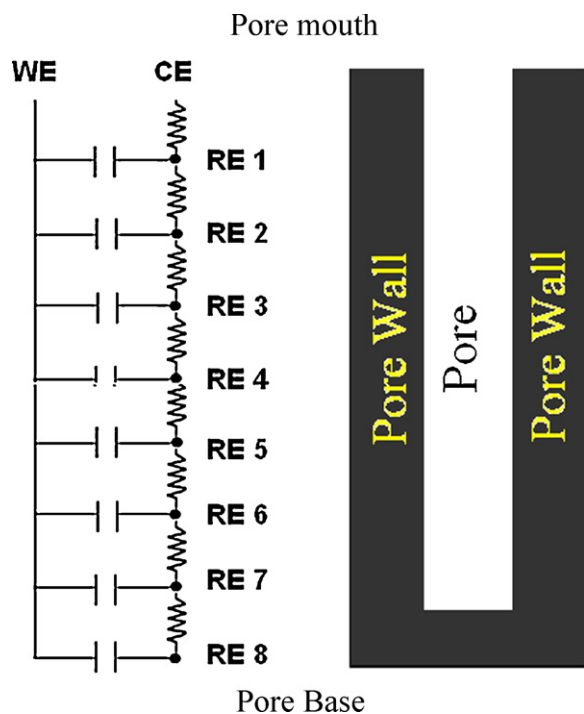


Fig. 1. Schematic of hardware circuit based on de Levie's transmission line model [1] (left) and an EC electrode pore (right).

that this can be used to aid in the identification of the mechanism of self-discharge in experimental systems. To do this, the de Levie transmission line is used as a model pore. Additionally, the Faradaic discharge of the pore is modelled in this transmission line through the application of a current which follows an activation-control profile.

Since the potential at the tip of the pore will be highest after charging, it would be expected that any Faradaic reactions would then happen preferentially at the tip of the pore, at least until the potential equalizes via CR. For this reason, in this work the potential profile was examined as an AC discharge was modelled at the pore tip, and CR was occurring throughout the pores. A transmission line hardware circuit of a model pore was used to first model CR, with no AC discharge, then an AC discharge was modelled with no CR, and finally both CR and an AC discharge were combined. The resulting potential profiles for each case were examined.

## 2. Experimental

### 2.1. System modelling

#### 2.1.1. Transmission line circuit

A hardware transmission line circuit was used as a model pore, based on the de Levie [1] transmission line model. A schematic of the hardware circuit used in the work is shown in Fig. 1. It consisted of eight parallel sections, with each section being composed of a resistor and capacitor in series. The resistors model the solution resistance down the pore which leads to the potential drop down the pore during charging/discharging (based on Ohm's law). The resistors could be set to a value between 0 and 300 k $\Omega$  (0–70 k $\Omega$  in 10 k $\Omega$  increments, 200, 300 k $\Omega$ ). The capacitors in the circuit model the capacitance of the double-layer at the electrode/electrolyte interface. Each capacitor was made up of a parallel combination of ten 10  $\mu$ F/6.3 V multilayer ceramic chip capacitors, for a nominal capacitance of 100  $\mu$ F. The capacitors in the hardware circuit could be shorted out and were brought to a zero charge state (0 V) prior to each experiment.

A Bio-Logic VMP3 multi-potentiostat was used to track the potentials at each terminal (RE 1–8). To do this the working electrode (WE) leads of the multi-potentiostat were linked together and connected to the WE point on the hardware circuit (as shown by WE in the schematic in Fig. 1) Similarly, the counter electrode (CE) leads were connected to the CE point. The reference electrode (RE) leads of each of eight channels were connected to points RE 1–8 of the hardware circuit.

The capacitor of the master channel (RE 1) was charged from 0.0 V to a chosen final potential between 0.2 and 1.0 V using a ramp rate of either 1 or 50 mV s<sup>-1</sup> and held for the desired time (0–150 min). When looking at CR only, this step was followed by opening the circuit and recording the potential of all eight capacitors of the transmission line circuit with time. For experiments utilizing an AC discharge, the ramp and hold steps were followed by the AC discharge experiment on capacitor 1 of the hardware circuit, and the potentials of the other 7 capacitors (RE 2–8) were recorded with time.

#### 2.1.2. Activation-controlled discharge

During self-discharge, the electrode is discharged through a Faradaic process occurring on the electrode surface, this Faradaic reaction causes charge to be removed from the surface at a rate which is governed by the kinetics of the Faradaic process (i.e. with a current/potential profile characteristic of the system). In order to simulate this Faradaic reaction (with activation-controlled kinetics) a current is drawn which has a current/potential profile which is characteristic of an activation-controlled Faradaic reaction. An experiment modelling an AC discharge was created using EC-Lab software (v.9.55 – Bio-Logic) and a 100-step galvanostatic cycling with potential limitation (GCPL) technique. This technique allows the user to draw a constant current until the system reaches a given potential limit, upon which a new constant current is drawn until the next potential limit is reached. For example, after ramping the potential to 1.0 V, the instrument will draw 6.484  $\mu$ A of current until the potential drops to 0.998 V, at which time the instrument will draw 6.237  $\mu$ A of current until the potential drops to 0.996 V, and so on. The potential limits and currents were chosen from a model, theoretical Butler–Volmer curve, based on a one-electron reaction with an equilibrium potential of 0.75 V, an exchange current density of  $5 \times 10^{-8}$  A, a symmetry factor of 0.5, at a temperature of 298 K. Because the multi-potentiostat was unable to draw currents below 0.1  $\mu$ A the AC discharge can only be modelled down to an overpotential of 50 mV, below which the value of the current required, as calculated from the Butler–Volmer equation, is at a lower value than the multi-potentiostat was capable of drawing (i.e. the currents that should be drawn at overpotentials less than 50 mV, based on the calculated Butler–Volmer curve, are lower than can be drawn by our instrument, thus these low overpotentials could not be modelled). The maximum current that could be drawn from the transmission line circuit was 7  $\mu$ A, as higher current than this would discharge the capacitors too rapidly, meaning that capacitor 1 would be completely discharged before CR had begun. Given the  $i_0$  used in this model, a 250 mV overpotential was the maximum used. The AC discharge was set to occur on capacitor 1 (RE 1) of the hardware circuit (Fig. 1), which represents the pore tip.

### 2.2. Electrochemical measurements

#### 2.2.1. Electrodes, cell and electrochemical measurements

Each working electrode was composed of a ca. 10 mg piece of Spectracarb 2225 carbon cloth (Spectracorp, BET surface area = 2500 m<sup>2</sup> g<sup>-1</sup>) mounted in a Teflon Swagelok PFA tube fitting in contact with Pt mesh contacted by a Pt wire, sealed in glass tubing. Electrolyte was prevented from leaking behind the Pt mesh by

a silicon gasket. Counter electrodes were fabricated from the same carbon cloth, wrapped with Pt wire for electrical contact. A standard hydrogen electrode (SHE) was used as a reference electrode, and this is the electrode to which all potentials in this paper are referenced.

Experiments were performed in a three-compartment, three-electrode glass cell in 1.0M H<sub>2</sub>SO<sub>4</sub> prepared from concentrated H<sub>2</sub>SO<sub>4</sub> (Sigma-Aldrich, 99.999% pure) and 18 MΩ water. The reference compartment was separated from the working electrode compartment via a luggin capillary. Nitrogen was bubbled through the working and counter electrode compartments prior to and during experiments to remove O<sub>2</sub> from the electrolyte. The experiments were conducted at 22 ± 3 °C. All measurements were performed using a Bio-Logic VMP3 multi-potentiostat. Data was collected using EC-Lab software.

Working electrodes were cycled between 0.0 and 1.0V vs. SHE using a sweep rate of 1 mV s<sup>-1</sup> for approximately one week (~350 cycles) prior to self-discharge measurements in order to bring the electrode to a steady-state whereupon no further changes in the shape or size of the cyclic voltammograms were seen. The 0.0 and 1.0V potential limits were used since at potentials outside of these limits undesirable, irreversible Faradaic reactions occur which destroy the carbon cloth electrode.

Self-discharge experiments were performed on carbon cloth electrodes in 1.0M H<sub>2</sub>SO<sub>4</sub> by first ramping the potential of the working electrode from 0V to the desired initial potential (0.9–1.0V) using a ramp rate of 1 mV s<sup>-1</sup>. The system was then switched into open-circuit configuration (zero current condition) and the potential of the working electrode was monitored over time.

### 3. Results and discussion

#### 3.1. Modelling charge redistribution only

It was previously shown that charging of the transmission line circuit resulted in a distribution of potentials down the length of the circuit (modelling the charging in a pore) and upon switching to open-circuit the charge redistributed until all capacitors in the circuit were at a common potential [3]. In this situation, the majority of the charge was moving down the circuit to charge the capacitors further down the circuit. This is termed CR<sub>down</sub>. This CR resulted in a linear potential profile in log *t* with a slope that was related to the initial charging potential [3]. This is similar to the self-discharge profiles of high surface area, porous carbon cloth electrodes, suggesting that CR is likely a significant factor in the self-discharge (Fig. 2). A previous study by the current authors shows that utilizing different charging rates (or hold times after charging)

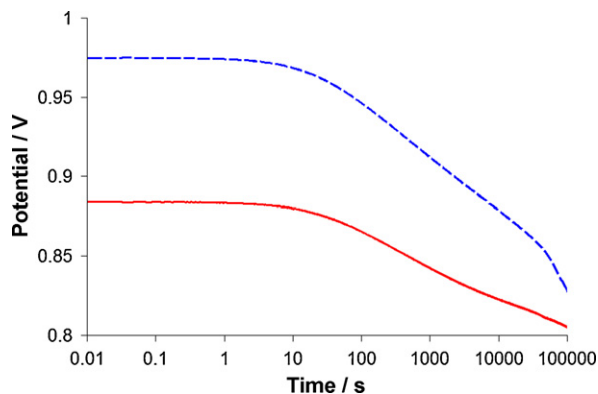


Fig. 2. Self-discharge profile resulting from charging to different initial potentials (1.0V(---); 0.90V(—)) of a carbon cloth electrode in 1 M H<sub>2</sub>SO<sub>4</sub>.

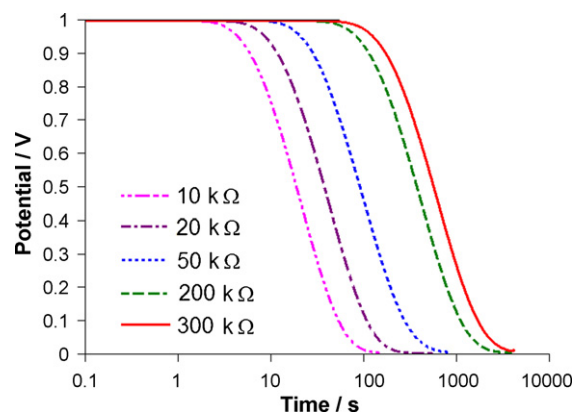


Fig. 3. Potential profile of capacitor 8 (pore base) of transmission line circuit with different resistances after all capacitors (1–8) were charged to 1.0V using a ramp rate of 1 mV s<sup>-1</sup>, and capacitor 1 was discharged to 0.0V.

ing) changes the self-discharge profile of the porous carbon cloth electrodes, as the amount of potential distribution, and therefore charge redistribution will depend on the charging rate (hold time) used [3].

Similarly, and not unexpectedly, it can be shown that if the entire circuit (pore) is brought to full charge (1.0V) and the pore tip (capacitor 1) is discharged to 0.0V the potential profile of the pore base (capacitor 8) also falls linearly with log *t* as charge redistributes back up the circuit (Fig. 3). Since in this case the majority of the charge is moving up the pore, this is termed CR<sub>up</sub>. Our previous work [3] and Fig. 3 show that regardless of the direction of CR in the model pore, the resulting potential profile is linear in log *t*.

#### 3.2. Modelling the activation-controlled discharge

In this work, the Faradaic process causing self-discharge has activation-controlled kinetics, and can therefore be modelled by the application of a current which is dependent on the potential as modelled by the Butler–Volmer equation. In order to first examine if the current/potential profile applied adequately models an activation-controlled reaction, the AC discharge experiment was first run on only capacitor 1 of the hardware circuit. Only the capacitor 1 was used in this simulation, as the AC self-discharge model (Eq. (1)), was developed for planar, not porous electrodes [4]. Fig. 4a shows the Butler–Volmer curve from which the AC discharge experiment was modelled, as described in Section 2.1.2, as well as the resulting Butler–Volmer curve obtained experimentally using the 100 step GCPL technique, with very good agreement between the two. Fig. 4b shows the potential profile of capacitor 1 in log *t* during the AC discharge, as well as the theoretical potential profile calculated from Eq. (1) using an empirically determined  $\tau = 3.3 \times 10^{-4}$ . Both the experimental and theoretical potential profiles (Fig. 4b) are linear in log *t*, as expected from the Conway model [4] for an activation-controlled self-discharge (Eq. (1)), with very good agreement between the two, a further indication that the AC discharge was working as expected. The slope of the experimental profile (110 mV per decade time) agrees well with the slope of the theoretical profile (112 mV per decade of time). Both slopes are slightly smaller than the predicted value from Eq. (1) (118 mV per decade of time, and 51 mV ( $RT/\alpha F$ ) when plotted as ln *t*), likely due to the non-ideality of the resistor and capacitor, as well as some residual influence of the plateau on the slope. Since only capacitor 1 is used to simulate the planar electrode for which the model was developed, there is no CR in this experiment, hence the good agreement between the model and the experimental. This confirms that the experiment was appropriately modelling an AC discharge.

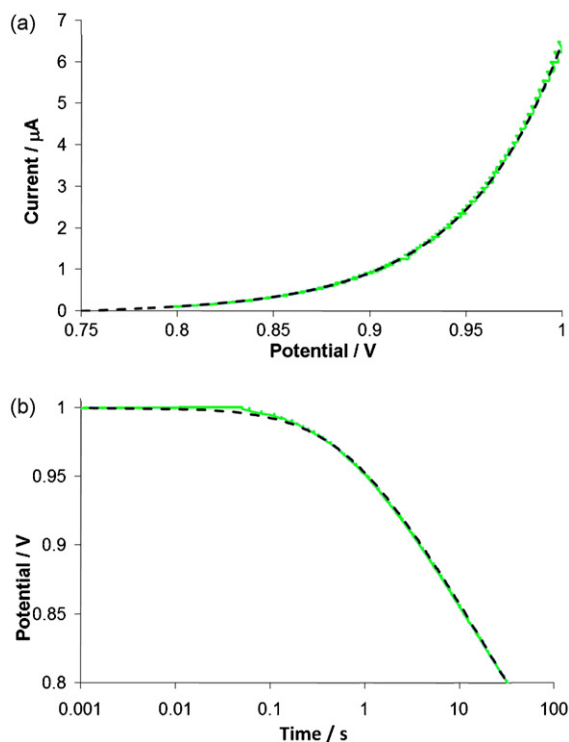


**Fig. 4.** Theoretical profile (dashed) and experimental profile of capacitor 1 of transmission line circuit (solid) during AC discharge plotted as: (a)  $I$  vs.  $E$  and (b)  $E$  vs.  $t$ .

### 3.3. Activation-control + charge redistribution up the circuit ( $AC + CR_{up}$ )

The AC discharge of the pore tip (capacitor 1) was then run with all capacitors present in the circuit, i.e. in the presence of CR. Again, the AC discharge models the spontaneous current that would flow during a Faradaic reaction occurring on the surface of the electrode during self-discharge. Thus, although a current is drawn during this experiment, this situation models what is happening in an electrochemical capacitor during open-circuit self-discharge measurements. To simplify the results, the experiments were first run with all capacitors in the circuit brought to a full charge of 1.0 V, thereby removing CR down the circuit ( $CR_{down}$ ), and having CR occurring only up the circuit ( $CR_{up}$ ) from capacitors 2–8 to capacitor 1. Fig. 5 shows the potential of capacitors 1–8 during an AC discharge on capacitor 1, after all capacitors in the circuit were

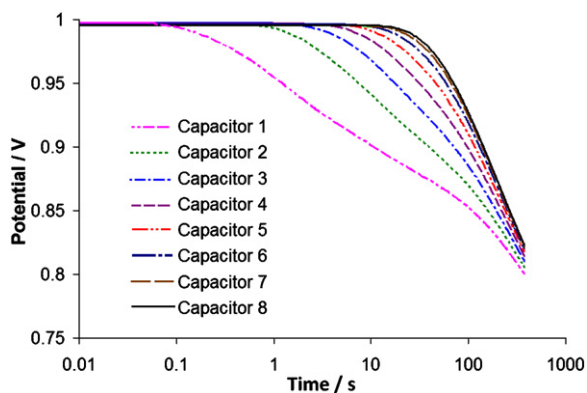


**Fig. 5.** Potential of all eight channels of transmission line circuit during AC discharge on capacitor 1 and  $CR_{up}$ , after all capacitors were brought to 1.0 V using a ramp rate of  $1 \text{ mV s}^{-1}$  and circuit resistances of  $50 \text{ k}\Omega$ .

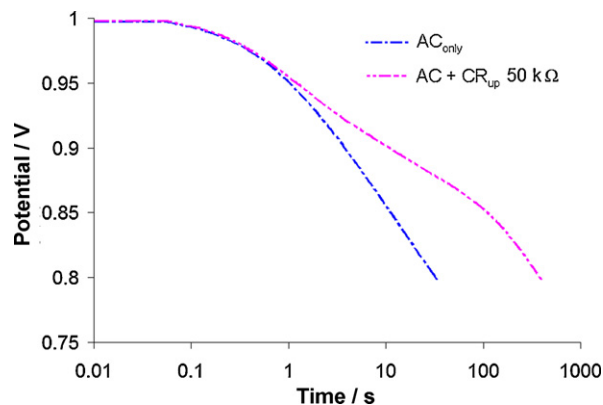


**Fig. 6.** Potential profile of capacitor 1 of hardware circuit ( $50 \text{ k}\Omega$  resistances and previously fully charged at  $1 \text{ mV s}^{-1}$ ) during AC discharge only, as well as AC discharge with CR back up the circuit.

brought to a potential of 1.0 V by using a hold time of 15 min (all resistances in the circuit were set to  $50 \text{ k}\Omega$ ). At  $50 \text{ k}\Omega$  resistance there is a significant difference in potentials among capacitors 1–8 during charging, and a hold time of 900 s (15 min) after the initial ramp allows all capacitors to reach full charge, removing the effects of CR down the circuit ( $CR_{down}$ ). However, there will still be CR back up the circuit ( $CR_{up}$ ) induced by the AC discharge of capacitor 1. This can be seen in Fig. 5 where the potential of capacitor 1 fell rapidly due to the AC discharge, followed by a drop in the potential of capacitor 2 (at ca. 1 s) as its charge passed back up to capacitor 1 (as potentials attempted to equalize). Over time, all eight channels eventually began to feed charge back up the circuit. With respect to a real pore, this data suggests that the regions near the pore tip react sooner (begin feeding charge up the circuit) than the regions further down the pore. This is consistent with what was expected based on previous results and on the de Levie model.

Fig. 6 shows the potential profile of capacitor 1 of the hardware circuit undergoing both AC discharge and CR back up the circuit ( $AC + CR_{up}$ ). For comparison, the AC discharge only ( $AC_{only}$ ) on capacitor 1, is also shown. Three distinct regions relating to AC and  $CR_{up}$  are seen in the potential profile of capacitor 1, the first being a curved region, followed by two linear regions. The first region (Region I) occurs at times below 1 s, the second (Region II) from 1 to 80 s has a slope of ca.  $46 \text{ mV}$ , and the third (Region III) at times longer than 100 s has a slope of ca.  $111 \text{ mV}$ .

In region I of Fig. 6 the curve corresponds almost directly with the curve showing AC discharge occurring when only capacitor 1 is in the circuit. This suggests that only the first capacitor is instrumental in determining the potential profile for  $AC + CR_{up}$  during this region. This occurs because the other capacitors have not yet begun to feed their charge back into capacitor 1, since the RC time constant for the circuit prevents CR from occurring that rapidly. As can be seen in Fig. 5, the potential of capacitor 2 was constant throughout the time duration of Region I (up to 1 s), since no charge is yet supplied back up the circuit to capacitor 1.

The onset of Region II can be attributed to CR becoming significant in the circuit as charge from capacitors 2–8 was fed back into capacitor 1 (Fig. 5), evidenced by the drop in potential for capacitors 2–8. The potential drop of capacitor 1 slowed with time as the charge removed by the AC discharge was replenished by the charge from capacitors 2–8. This recharging of the first capacitor resulted in the decrease in slope seen in Region II for capacitor 1 in Fig. 6. This suggests that the slope of the self-discharge profile in porous experimental systems will be affected by the presence of CR, resulting in a shallower slope than would be expected for the purely AC profile.

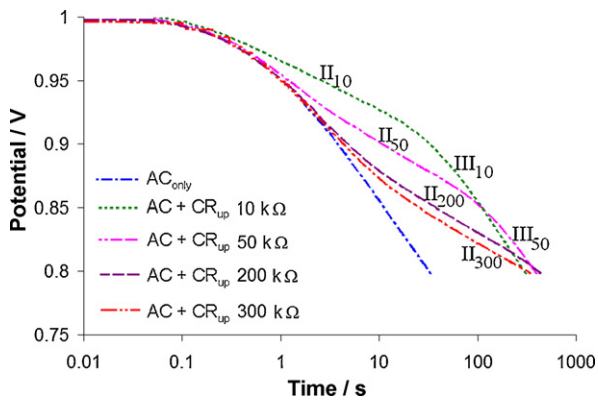


**Fig. 7.** Potential profile of capacitor 1 of the transmission line circuit (previously fully charged at  $1 \text{ mV s}^{-1}$ ) with AC discharge and  $\text{CR}_{\text{up}}$  the circuit for different resistances. Labels show Region II and III for each resistance.

The slope in Region III correlates well with the slope obtained for only AC with no CR. At this point there was only a small potential difference between capacitors 1–8 (see Fig. 5), and therefore  $\text{CR}_{\text{up}}$  due to potential distribution had ended, as the charge being fed back into capacitor 1 was minimal. Therefore, in Region III the AC is dominating the slope. It is important to note here that for experiments with both AC and  $\text{CR}_{\text{up}}$ , the CR will never truly be over, as the charge removed from capacitor 1 by the AC discharge will be replaced by charge from the capacitors further down the circuit. As a result, the slope obtained may differ from that of the AC only profile, as the rate at which the charge in capacitor 1 will be replaced (which will affect the slope) will be limited by the resistance through which the charge has to travel.

This model suggests that in a real system with an AC self-discharge occurring on a highly porous electrode, CR likely affects the slope of the self-discharge curve for significant times. This then explains why with these high surface area electrodes there is no consistency in the slope with self-discharge potential, such as that seen with nickel-oxide [5]. The model also suggests that the completion of CR will result in a change of slope, and this change can be used to determine the length of time for CR in these systems. This will be shown in Section 3.5.

### 3.3.1. Modelling the effect of pore diameter/electrolyte conductivity

As the resistance of the circuit was increased (which models either a decrease in ionic strength of an EC electrolyte or a smaller cross-sectional area of pore) the effects of CR also increased, due to the increase in the RC time constant of the circuit. During charging of the circuit with high resistance values, the capacitors 2–8 did not climb to as high of a potential as they did with lower resistances and there was an increased amount of CR down the circuit. Nevertheless, as can be seen in Fig. 7, regions I and II (as described above) remain in the self-discharge profile at each different resistance, although Region III is not seen at high resistances, due to experimental limitations described below.

Again, in Region I all curves correspond with one another and, regardless of the number of capacitors in the circuit, in this region all systems behave as if only one capacitor is available. For increased resistances the charge will move more slowly through the circuit, as the RC time constant increases, and therefore CR will take longer and will initiate more slowly. This is evident in Fig. 7, as the time of Region I is directly related to the resistance in the circuit, where this region is very short for low resistances (e.g.  $10 \text{ k}\Omega$ , with a time of  $0.2 \text{ s}$ ), and very long for high resistances (e.g.  $200 \text{ k}\Omega$  with a time of  $2 \text{ s}$ ). At low resistances, capacitor 2 can very quickly begin to recharge capacitor 1 since only a small resistor hinders this current

flow. This suggests that the length and/or presence of Region I in the self-discharge profile of porous EC electrodes may be a gauge to the incremental solution resistance in the system, as a system with a very low incremental solution resistance will exhibit little to no curved Region I, since the current can very easily pass from surface area deeper in the pore up to the pore tip. Conversely, the significant presence of a curved Region I may suggest a high incremental solution resistance.

Once CR began in each circuit, corresponding to Region II, the typical linear profile was seen with a shallow slope. At low resistances (e.g.  $10 \text{ k}\Omega$ ) charge moved very quickly through the circuit, meaning that the CR required a much shorter time. This can be seen in Fig. 7 as the potential remained higher for longer with lower resistance, as charge was quickly and easily passed up the circuit to capacitor 1 to keep this capacitor charged. The slope of Region II is independent of resistance (Fig. 7). This is not unexpected as neither the slope of the  $\text{AC}_{\text{only}}$  result nor the CR only is dependent on resistance, when plotted as  $\log t$  (see Fig. 3); however, the slope in normal time plot is smaller for higher resistances because with higher resistances the charge moves more slowly through the circuit. In fact, for high resistances (e.g.  $200$  and  $300 \text{ k}\Omega$ ) CR was much slower and required the entire AC discharge time, and there was no region in which the slope is controlled solely by AC (no Region III). As mentioned above, at high resistances (e.g.  $200 \text{ k}\Omega$ ) the CR takes much longer, and in fact continues beyond the time required to complete the AC discharge.

### 3.3.2. Modelling the effect of pore length

Increasing the number of capacitors in the hardware circuit is analogous to modelling a longer pore. As the number of capacitors in the circuit was increased (i.e. for longer pores) the effect of CR also increased. This is because for each additional capacitor added to the circuit a resistor is also added, which creates a potential difference between the capacitors during charging, leading to CR. As the number of capacitors (and therefore resistors) in the circuit increases, this potential difference developed between the capacitors at the far ends of the circuits will be amplified, leading to increased effects of CR on open-circuit. This is analogous to the real situation in a porous electrode, as generally, higher EC electrode areas are achieved by using materials with longer and smaller pores. These longer pores result in longer paths (more solution resistance) through which the current must flow, resulting in a situation equivalent to using more resistors in the transmission line circuit. Fig. 8 shows the potential profile of capacitor 1 as the number of the capacitors in the circuit was increased. As more capacitors were added to the circuit the length of time for CR increased, as there is now more charge available to feed back

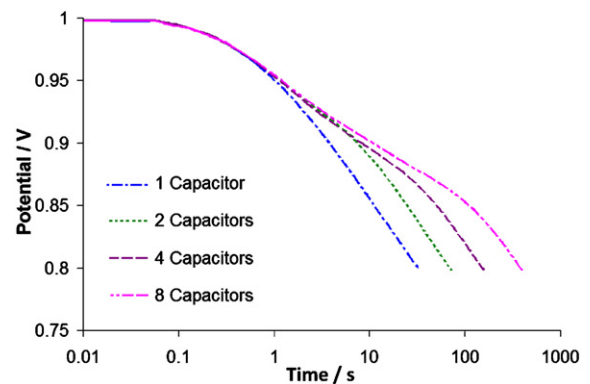


**Fig. 8.** Potential profile of capacitor 1 of transmission line circuit ( $50 \text{ k}\Omega$  resistances and previously fully charged at  $1 \text{ mV s}^{-1}$ ) with AC discharge and  $\text{CR}_{\text{up}}$ , using different number of capacitors.

into capacitor 1 from each additional capacitor added to the circuit.

The length of Region I is independent of the number of capacitors in the circuit, which makes sense as Region I is controlled by only the first capacitor in the circuit, as mentioned above, since capacitors 2–8 have not yet contributed any charge due to the RC time constant. Increasing the number of capacitors in the circuit increased the total amount of charge present in the circuit, and also increased the RC time constant, causing CR to last longer. A longer CR results in a longer Region II.

For 50 k $\Omega$  resistances, Region III is almost solely controlled by the AC discharge. However, as mentioned previously, although in Region III the potential difference among capacitors 1–8 is minimal, CR back up the circuit (CR<sub>up</sub>) is never truly over, but the rate of charge transfer is dependent on resistance, and CR is slower in Region III with high resistances. This is evident in Fig. 8 as a potential drop from 0.85 to 0.80 V requires ca. 20, 45, 100, and 300 s for 1, 2, 4, and 8 capacitors, respectively.

### 3.4. Charge redistribution down, up and activation-control (AC + CR<sub>down</sub> + CR<sub>up</sub>)

In a real, highly porous electrode system, it is unlikely that the full surface will be completely/fully charged during a commercially viable charging ramp. Thus, in this case, CR both up and down the pore (CR<sub>up</sub> + CR<sub>down</sub>) may be expected to occur. To model this more realistic situation the AC discharge of the pore tip (capacitor 1) was then run in the presence of CR both up and down the circuit (CR<sub>up</sub> + CR<sub>down</sub>). Here the potential of capacitor 1 was ramped from 0 to 1.0 V prior to the AC discharge, while the potential on capacitors 2–8 remained at some value below 1.0 V due to the added resistance down the circuit. Fig. 9a shows that similar to the AC + CR<sub>up</sub> case, three distinct regions are seen in the potential profile of capacitor 1 undergoing an AC discharge in the presence of CR both up and down the circuit (AC + CR<sub>down</sub> + CR<sub>up</sub>).

Again, the potential profile in Region I is controlled by capacitor 1 as described above, and therefore Region I is unaffected by the presence of CR down the circuit (CR<sub>down</sub>). This is because the RC time constant for the circuit prevents CR from happening this quickly, and all charge removed from capacitor 1 in Region I was a result of the AC discharge. This can be seen in Fig. 9b, where the potential of all capacitors 2–8 remained unchanged through this region.

When both CR<sub>up</sub> and CR<sub>down</sub> are occurring, Region II depends on both the direction, as well as the amount of CR. This leads to a more complex profile and Region II loses its linearity, as seen in Fig. 9a. For 50 k $\Omega$  resistances, the potentials of capacitors 2–8 were significantly lower than 1.0 V (the potential of capacitor 1) after charging, as seen in Fig. 9b. Because of this, capacitors 2–8 were unable to contribute charge to capacitor 1 until the potential of capacitor 1 dropped to a value below that of capacitors 2–8, meaning there was no CR up the circuit (CR<sub>up</sub>) at these short times. However, at ca. 1 s, the potential of capacitor 1 fell below that of capacitor 2 (Fig. 9b) resulting in the initiation of CR<sub>up</sub>, as capacitor 2 began passing charge to capacitor 1. A small amount of charge from capacitor 2 also went into charging capacitor 3 whose potential increased slightly, indicating that CR<sub>down</sub> had also begun to occur. This CR<sub>down</sub> can be most easily seen with the potential of capacitor 8 which climbed significantly as charge from the other capacitors was passed down the circuit into capacitor 8. With CR only happening back up the circuit (AC + CR<sub>up</sub>), as discussed above, the slope in Region II was decreased (compared to the slope for only AC) as charge from capacitors 2–8 was fed back into capacitor 1. With CR now occurring in both directions, i.e. up and down the circuit (CR<sub>up</sub> + CR<sub>down</sub>), Region II has lost its linearity as the various processes (AC, CR<sub>up</sub> and CR<sub>down</sub>) compete. The amount of charge

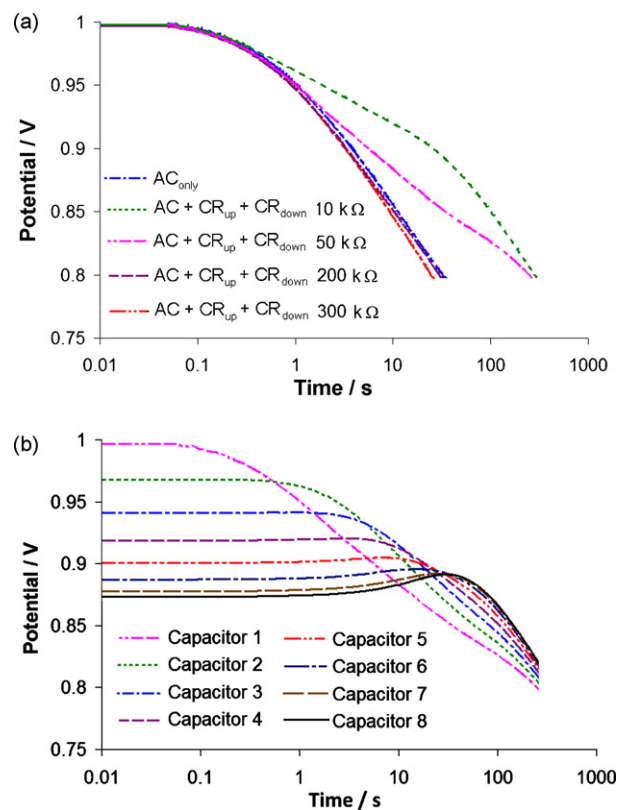


Fig. 9. a) Potential profile of capacitor 1 of transmission line circuit (charged at 1 mV s<sup>-1</sup>, no hold time) with AC in the presence of charge redistribution up (CR<sub>up</sub>) and down (CR<sub>down</sub>) the circuit. b) Potential profiles of each capacitor for transmission line circuit using 50 k $\Omega$  resistances (charged at 1 mV s<sup>-1</sup>, no hold time).

that capacitors 2–8 contributed to recharging capacitor 1 was less than previously seen with AC + CR<sub>up</sub>, as the potential of capacitors 2–8 was now lower. This then resulted in a slope in Region II which was less than that for AC<sub>only</sub> but larger than that for AC with CR<sub>up</sub> only (AC + CR<sub>up</sub>). At high resistances (e.g. 200 k $\Omega$ ) there was a very large potential difference developed among capacitors 1–8 upon charging, and as a result there was a large amount of charge redistributed from capacitor 1 to capacitors 2–8 in Region II. As a result of charge being removed from capacitor 1 due to the AC discharge as well as from capacitors 2–8 due to CR down the circuit (CR<sub>down</sub>), the potential of capacitor 1 dropped very quickly in Region II, and the slope was steeper than for AC only. The length of Region II is approximately the same for the curve with AC in the presence of only CR back up the circuit (AC + CR<sub>up</sub>), compared to having CR in both directions (AC + CR<sub>up</sub> + CR<sub>down</sub>).

### 3.5. Comparison with self-discharge profile of highly porous electrodes

Experiments are underway in the authors' laboratory to study the self-discharge profile of highly porous electrodes under various conditions to compare with the model presented here. Fig. 2 shows the self-discharge profile of a porous carbon electrode in 1 M H<sub>2</sub>SO<sub>4</sub>. As can be seen in this figure, there is a plateau immediately followed by a relatively linear region. This is similar in shape to the profile evidenced at low resistance (10 k $\Omega$ ) in Fig. 7. The absence of a sharply curved Region I may suggest that the incremental solution resistance is fairly low. This would be consistent with the high proton content (ca. 1 M) in this electrolyte. Region II can be easily seen, between 60 and 30,000 s. This region has a shallow slope suggesting that CR is likely occurring possibly coupled with an AC

self-discharge. This is supported by the increase in slope (Region III) seen at 60,000 s (17 h) where presumably the CR ends and the AC self-discharge discharges the electrode rapidly. This data suggests that CR takes significantly longer than the 100 s previously suggested [2], and can therefore not be ignored during mechanistic studies. Initial analysis of the shape of Region II suggests that CR may only be occurring in one direction (likely down the pore), as indicated by the linearity of this region.

#### 4. Conclusions

A de Levie transmission line hardware circuit was used to model the self-discharge profile which occurs on a highly porous electrochemical capacitor electrode in the presence of an activation-controlled discharge. The model showed that this situation results in three distinct regions in the self-discharge profile. The first region corresponds to the profile relating to a purely activation-controlled profile. This is due to the fact that the charge redistribution, which would be expected to occur on the porous electrode, requires some time to initiate, and has not yet begun to occur in this region. The presence and length of this first region (Region I) depends on the incremental solution resistance in the pore and can be used to predict the solution resistance in real electrochemical capacitor systems. Region II in the self-discharge profile has a shallower slope than expected for an activation-controlled self-discharge profile. This shallower slope is due to the charge redistribution in the circuit, where the capacitors down the circuit (or surface area deep in the pores) begin to feed charge back up to the first capacitor (pore mouth) where the activation-controlled discharge is occurring. The profile of the first capacitor does not, therefore, fall as quickly as would be expected if this recharging were not occurring. Increasing the resistances and capacitance in the model pore (akin to modelling narrower, longer pores or lower electrolyte conductivities) increases the length of

Region II. Upon completion of the charge redistribution, the slope of the self-discharge profile again increases (Region III), providing a means to determine the duration of the charge redistribution in experimental systems.

When the self-discharge profile of a highly porous carbon electrode was examined in 1 M H<sub>2</sub>SO<sub>4</sub>, the predicted distinct regions were observed. A very short, nearly absent, Region I was seen, suggesting a very low incremental solution resistance, which correlates nicely with the high concentrations of protons in this electrolyte. Region II is very long for this experimental system. Again, this correlates very nicely with what might be expected, as long narrow pores (such as those in the carbon examined) would be predicted to have a very large RC time constant, as the cumulative resistance and surface area would be very high in these pores. From the self-discharge profile, it is suggested that charge redistribution requires at least 60,000 s (ca. 17 h) to complete. This is much longer than had been previously predicted in the literature [2].

#### Acknowledgements

The authors would like to acknowledge the support of the Natural Sciences and Engineering Research Council (NSERC) for funding of this project. Additionally, the authors gratefully acknowledge Brian Miller, Dept. of Chemistry, Dalhousie University for building the hardware circuit.

#### References

- [1] R. de Levie, *Electrochim. Acta* 8 (1963) 751–780.
- [2] W. Pell, B.E. Conway, W. Adams, J. Oliveira, *J. Power Sources* 80 (1999) 134–141.
- [3] J. Black, H.A. Andreas, *Electrochim. Acta* 54 (2009) 2574–3568.
- [4] B.E. Conway, W. Pell, T. Liu, *J. Power Sources* 65 (1997) 53–59.
- [5] J. Niu, B.E. Conway, *J. Power Sources* 135 (2004) 332–343.